# Dynamic Tactile Sensing: Perception of Fine Surface Features with Stress Rate Sensing

Robert D. Howe and Mark R. Cutkosky

*Abstract*—**Most robot tactile sensing research has focused on the static perception of object shape with tactile array sensors. In contrast, dynamic tactile sensing is presented, which is defined as sensing *during* motion for perception of high spatial and temporal frequencies. Applications include sensing fine surface features and textures and monitoring contact conditions for dextrous manipulation. One type of dynamic tactile sensor, the stress rate sensor, is described in detail here. It uses piezoelectric polymer transducers to measure the changes in stress induced in the sensor's rubber skin as it traverses small surface features and textures. The signals are interpreted with the aid of a solid mechanics model of the contact interaction and a linear deconvolution filter. Experimental verification of the sensor's performance, including the detection of surface features only 6.5 $\mu$m high, are presented.**

## I. Introduction

FOR PEOPLE, perception of the world through touch is inseparable from motion. If you place your hand against a textured surface such as wood or cloth and hold it still, it is very difficult to identify the texture. But as soon as you begin to explore the surface, moving your fingers lightly over it, you can describe it in detail. Not only is motion indispensable, but active, purposeful movements by the observer are necessary for the resulting tactile stimuli to be ascribed to an object, rather than attributed to unconnected sensory events on the skin [29].

This paper describes a new approach to tactile sensing which takes advantage of sensor motion. Most tactile sensing research has emphasized finding the shape of objects using touch. In contrast, dynamic tactile sensors are designed to provide information about local conditions at the contact between a robot finger and its environment. Because these sensors can be scanned across a surface and because they respond to time derivatives of physical quantities, they can measure higher spatial and temporal frequencies than conventional tactile sensors. The information they provide extends the range of parameters that can be sensed in tactual exploration and is important for robust, flexible control of manipulation.

One type of dynamic tactile sensor, the skin acceleration sensor, is sensitive to minute vibrations at the finger-object contact. It is useful in manipulation for detecting changes in contact conditions such as the onset of slip. The construction and use of this sensor is described in detail in [12], [13]. Another sensor, the stress rate sensor, is described in this paper. It uses a piezoelectric polymer transducer to measure the changes in stress induced in the sensor as it slides over fine surface features. The interaction between the sensor and the surface is analyzed with the aid of a solid mechanics model. Linear inverse filtering is used to find the distribution of surface loading from the stress rate signal. Tests of the sensor's performance are reported, and extensions and applications are also considered.

Manuscript received February 4, 1991; revised April 23, 1992.

This work was supported by the National Science Foundation under Grants DMC8552691 and DMC8602847.

R. D. Howe is with the Division of Applied Sciences, Harvard University, Cambridge, MA 02138.

M. R. Cutkosky is with the Design Division of the Mechanical Engineering Department, Stanford University, Stanford, CA 94305.

IEEE Log Number 9207357.

### A. Previous Work

The primary focus of robot touch sensing research has been the determination of object shape. The sensors used are typically arrays of pressure sensors with about $10 \times 10$ elements on 2 mm centers (e.g., [1], [9]). Most work on tactile sensing with "motion" has been concerned with scheduling moves between static array sensor readings for the purpose of object recognition (e.g., [6], [11]). In emulation of human haptic behavior, some work has appeared on the use of hand movements to learn about object properties such as contour tracing and compliance measurement (e.g., [17], [28]).

A few touch sensors have appeared for use during motion. Buttazzo, Dario, and Bajcsy [2] have attached a plastic "fingernail" to the back of a robot finger. A piezoelectric element at the base responds to variations in surface height as the nail is dragged over an object. It may be possible to analyze the signal from this sensor to find details of the surface finish, but because it does not form part of the gripping surface of the finger it cannot be used during manipulation. Patterson and Nevill [23] have developed an induced vibration sensor for recognizing small shapes and textures. Large areas of piezoelectric film are excited by vibrations induced in a ridged rubber skin when the sensor slides over a surface. Because of the complicated interaction between the sensor and test surface, analysis is difficult and the signal varies greatly with small displacements of the test object. However, repeatable results are obtained under controlled conditions and the sensor is able to identify test objects from among a list of candidates using pattern recognition techniques on the power spectrum of the signal.

This work addresses the detection of fine surface features and textures, which has also been a subject of considerable interest in computer vision. Vision can provide global information at a distance, since information is radiated to

1042-296X/93$03.00 © 1993 IEEE

the sensor from the environment. Touch, on the other hand, provides only local information and requires contact between the sensor and the environment, so movement is an essential part of tactile sensing. It also provides important mechanical information such as compliance, friction, and force direction and magnitude that is impossible to determine visually. Touch is immune to the perspective distortions, scale variations, and shadows that complicate the processing of visual information.

### B. Dynamic Tactile Sensing

In this work dynamic tactile sensing is defined as tactile sensing *during* motion, in contrast to the sequences of static pressure measurements produced by most tactile sensors. The differences between static and dynamic sensing include:

- *Derivative Information:* Some manipulation and perception tasks require information that is the time derivative of static sensor data, and the transducers for sensing derivative quantities can be very different from the ones for static quantities. Thus an accelerometer can be far more effective than a displacement sensor for measuring small, fast displacements [12].
- *Scanning:* To sample a surface without motion requires a two dimensional array of sensors, while a single line of sensors can scan a surface to sample it. This means that high spatial resolution can be obtained without a large number of sensors.
- *Tangential Stresses:* Movement produces tangential stresses which can provide more information about surface asperities and textures.
- *Surface Changes* - As the sensor moves against a surface, small changes in the surface can occur that provide considerable information. For example, we learn that a surface is gritty or fuzzy or velvety from the way the elements of the surface move as we stroke our fingers over it.
- *Friction:* To assess the frictional properties of a surface requires movement. The coefficient of friction or its variation with sliding speed obviously cannot be determined from static measurements.
- *Relative Measurements:* Perception often does not require good absolute sensitivity but sensitivity to small differences in stimulus. To detect a small difference in surface properties between adjacent points, static sensing requires finding the difference between adjacent sensors. In active sensing, small differences in adjacent surface areas are presented to a single sensor in rapid succession. This minimizes the need for calibration and the effects of sensor drift.
- *Mechanical Transients:* During dextrous manipulation small vibrations are produced by events such as the onset of slip between a robot finger and the grasped object or by contact between the object and other surfaces in the environment. These events signal important changes in the state of the manipulation system. Dynamic tactile sensors are able to detect the mechanical transients that accompany these events, which improves the robustness of robotic manipulation [13].

## II. Sensor Design

To sense fine surface features and textures requires a special-purpose sensor: traditional tactile array sensors lack the required spatial resolution and sensitivity. For the reasons enumerated above, this can be advantageously accomplished with a moving sensor that is scanned over the surface of interest. The presence of motion leads naturally to the measurement of stress and strain rates. The interaction between a surface and a tactile sensor produces stresses and strains in the sensor, which are the quantities that virtually all robot tactile sensors to date have sensed. However, as a sensor moves along a surface, the stress and strain distributions within the sensor change, and these changes can be measured directly as the stress or strain rate. Integration of these rates gives the total stress or strain on the sensor, but the rates themselves are also of interest.

The stress rate sensor is designed to form part of a robot finger for use during manipulation and exploration. A cross section of a robot finger incorporating the sensor is shown in Fig. 1. The finger is roughly cylindrical in shape with a diameter of about 25 mm. The core consists of the rigid robot finger structure, around which is wrapped a thin silicone rubber "skin." Between the rubber skin and the rigid core is a compliant layer of foam rubber several millimeters thick; a fluid could also be used in place of the foam. This compliant layer is of great importance. If the sensor surface is stiff (e.g., made from hard rubber), then control errors during surface tracking will result in large changes in the contact force, swamping the relatively small signal from fine surface features. A stiff sensor will likewise couple vibrations in the robot drive train to the sensing element.

On the other hand, a soft surface on the sensor will provide large contact areas, improving grasp stability and control of contact forces. But a soft outer skin will also be fragile and easily damaged. Thus the sensor is constructed with a thin outer skin of relatively tough rubber and an inner layer of soft foam rubber. Besides increasing durability, the use of a hard skin increases local stresses in the surface of the sensor, which improves performance of the stress rate sensor, as described in section A. below.

Various textures have been molded into the surface of the rubber skin. An extremely smooth surface (local roughness less than about 1 $\mu$) can produce a very large coefficient of friction, and this adhesive behavior causes stick-slip motion as the sensor slides over smooth surfaces [26]. The stress rate sensor is very sensitive to these oscillations, so this skin texture is not generally useful. A mat finish (local roughness on the order of a few tens of microns) has a substantially lower coefficient of friction and can slide evenly over smooth surfaces. This is the skin texture we used for the tests reported here.

Another texture consists of parallel ridges a few hundred microns apart and up to a few hundred microns high, reminiscent of human fingerprints. This texture produced good signals on smooth surfaces without the stick-slip problem of the smoothest texture. Fearing and Hollerbach have determined that ridges increase the magnitude of the subsurface strains in the sensor, which improves detectability [10]. Cutkosky,

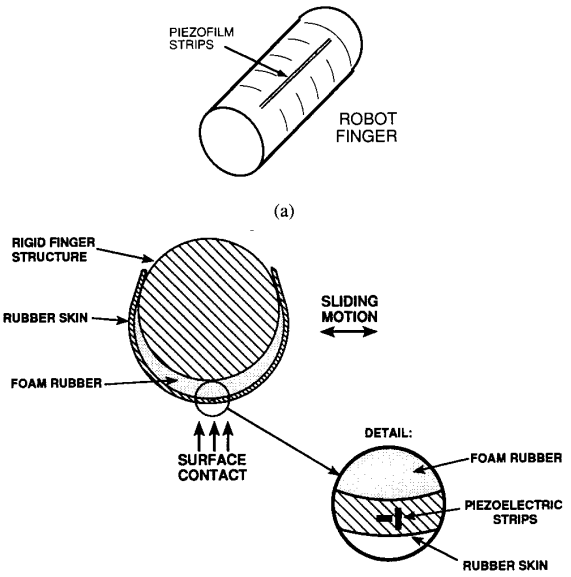


Fig. 1. Prototype sensor configuration. (a) Robot finger with stress rate sensor elements in contact surface. (b) Cross section of a robot finger showing compliant layer between rigid finger structure and flexible rubber skin.

Jourdain, and Wright have noted that ridges act like tire treads to provide good friction when the contact is wet [4]. This texture was not used in the experiments reported here because ridges complicate the analysis of the interaction of the sensor with the test surface.

### A. Piezoelectric Transducers

The piezoelectric transducers used in this sensor are made from polyvinylidene fluoride ($PVF_2$) film, a flexible polymer with very good piezoelectric response [24]. Strips of piezofilm 28 $\mu$ thick, 0.5 to 1 mm wide, and 35 mm long are molded into the rubber skin about 0.75 mm beneath the outer contact surface. For the tests reported here the piezofilm strips were desensitized by heating everywhere except for a length of about 8 mm under the center of the sensor skin, in order to lessen sensitivity to edge effects near the borders of the skin. A thin layer of metallization is applied to the outer faces of the film to collect the generated charge and to provide electrical contact. Electromagnetic shielding is provided by laminating two piezofilm strips together "face-to-face," with the outer surfaces of the laminated element grounded. Additional shielding is provided by a grounded conductive layer just under the surface of the rubber skin.

The piezoelectric film acts as a capacitor on which charge is produced in proportion to the stress applied to the film. The transduction constant between stress and charge is different in each direction within the film, so the constants of proportionality can be written as a vector $\mathbf{d} = [d_1 d_2 d_3]^T$ (see Fig. 2). The charge $q$ developed on the piezofilm can then be expressed in terms of the applied stresses $\sigma = [\sigma_1 \sigma_2 \sigma_3]^T$ as the dot product

$$q = A\,\mathbf{d} \cdot \sigma \tag{1}$$

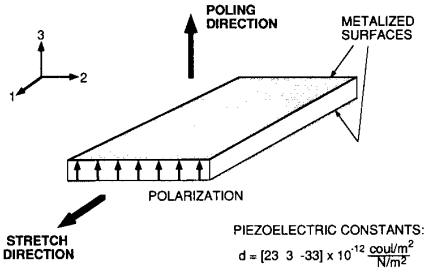


Fig. 2. Piezofilm orientation and sensitivity. Piezoelectric constants for the film used in these experiments are from [24].

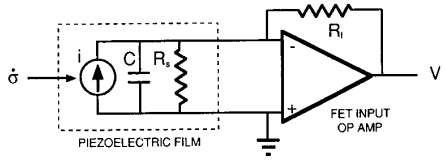


Fig. 3. Current-to-voltage amplifier connected to piezofilm elements.

where $A$ is the film strip area and the stress vector is assumed constant across the film strip.

Piezoelectric transducers are most often used with charge amplifiers so that the output voltage signal is proportional to the measured stress. However, for this sensor the piezofilm strip is connected to a FET-input operational amplifier configured as a current-to-voltage converter (see Fig. 3). Since current $i$ is the time rate of change of charge, the output voltage $v$ is proportional to the time rate of change of the stress, or to the stress rate:

$$v = \frac{dq}{dt} R_f = A R_f \mathbf{d} \cdot \frac{d\sigma}{dt}. \tag{2}$$

Here $R_f$ is the op amp feedback resistance, typically 1 M$\Omega$. In this configuration the op amp effectively servos the voltage developed across the film to zero. Since the voltage across the piezofilm is minimized, inaccuracies due to charge leakage through the internal resistance of the film are negligible and the required transducer impedance is far lower than for a conventional charge amplifier. Furthermore, the sensor has little low-frequency and no dc response, so it is immune to saturation due to drift and pyroelectric effects, which are common problems with piezoelectric tactile sensors [2]. The sensor signal can then be integrated in subsequent processing stages to find the total stress, but the stress rate signal itself is also of interest since it provides large, fast signals indicating changes in contact stresses during manipulation and exploration.

## III. Analysis

One of the prime functions of the stress rate sensor is to provide information about fine features on surfaces in the environment. However, the sensor elements are located at some depth beneath the surface of the rubber skin and the piezofilm responds to all three components of the subsurface stress, so the sensor signal does not directly reveal the desired surface information. It is therefore necessary to analyze the

mechanical interaction between the sensor and the test surface to find the relationship between the surface stimulus and the subsurface stresses at the sensor elements. Then the piezofilm response to these stresses must be determined. This analysis is presented in the first part of this section, and makes use of the theory of elasticity and the properties of the piezoelectric polymer.

On the basis of this analysis it is possible to calculate the sensor output given a known surface feature, but obviously what we need is just the opposite, i.e., to calculate the surface conditions from the sensor signal. Since the elasticity theory relating the surface conditions and the signal is linear, a linear deconvolution filter can be used to "invert" the analytic result so that the surface information can be extracted from the sensor signal. The second part of this section develops the signal processing algorithms for performing the inversion.

### A. Solid Mechanics

This section develops a model for the mechanical interaction between the sensor and test surface during sliding. The analysis is based on linear elasticity theory, particularly plane strain contact mechanics. Timoshenko and Goodier [30] and Johnson [16] cover the development of the theory used in this section. In previous work on tactile sensing, Phillips and Johnson [25] used a similar approach to model the response of mechanoreceptor afferents in monkey fingertip skin. Fearing and Hollerbach [10], Fearing [8], [9] and Speeter [27] have developed linear elastic models to describe strain-based robot tactile array sensors.

*Model Assumptions:* In constructing a model of a complex process such as the sliding interaction of the stress rate sensor and a test surface, a number of simplifying assumptions must be made to keep the model tractable. Since the sensor element is located near the surface of the skin and its dimensions are small compared to the size of the finger, the rubber sensor skin is idealized as a homogeneous, isotropic infinite elastic half space. Because the elastic modulus of the $PVF_2$ is substantially higher than the rubber of the skin ($3 \times 10^9$ N/m$^2$ versus $7 \times 10^5$ N/m$^2$), we will assume that the piezofilm responds to local stresses rather than strains, as has been assumed in previous tactile sensor models (e.g., [9]). The value for Poisson's ratio will be taken as exactly 1/2, in accordance with the incompressibility of rubber and as confirmed experimentally for the rubber used in these tests.

To reduce the complexity of the model and the sensor construction for this preliminary study the model also assumes plane strain conditions, so there is no variation in the surface shape and contact conditions along the entire width of the sensor (i.e., in the direction parallel to the test surface and perpendicular to the direction of travel).[1] Thus all cross sections of the sensor and test surface are identical, and the elastic material cannot deform out of the plane of each cross section. It is also assumed that the finger slides smoothly and at a constant height across a relatively flat surface, producing only small strains in the fingertip. "Plucking" or catch-snapback of the sensor skin due to surface asperities will be treated as a noise source in signal processing considerations. Sliding speed (typically 1–10 cm/s) is presumed constant and small enough that dynamic effects such as wave propagation and viscoelasticity can be ignored.

These assumptions represent a clear oversimplification of the actual situation. The sensor skin is closer to a flexible membrane than an elastic half space, and it is far from homogeneous and isotropic since it contains piezofilm elements and a shielding layer with varying modulus. Likewise, the smooth sliding assumption is more or less true, depending on the particular surface roughness and frictional properties encountered. It would also be useful to relax the plane strain condition so that arbitrary surface shapes could be perceived. However, the final evaluation of the utility of this model comes through comparison with experimental results. As the subsequent sections show, this model is successful in predicting the sensor response and provides satisfactory results in many situations. Furthermore, this model represents a useful starting point for the development of high resolution near-surface tactile sensors. It provides physical insight into the sensor's functioning, indicates improvements to the sensor design, and suggests further lines of investigation into tactile sensing of fine surface features.

### B. Coordinates and Sliding

Suppose that a fingertip composed of a linear, isotropic elastic material has a small stress rate sensing element embedded near its surface (see Fig. 4). The coordinate system attached to the test surface is defined so that the $z$ direction is normal to the surface while the finger slides in the $x$ direction with sliding velocity $u = dx/dt$. The sensor is located at a depth $z_0$ and experiences normal stresses $\sigma(x, y, z_0) = [\sigma_x(x, y, z_0), \sigma_y(x, y, z_0), \sigma_z(x, y, z_0)]^T$, where a positive value denotes tension. Under the smooth sliding conditions assumed above, the stress distribution in the fingertip is fixed with respect to the surface coordinate system, so the sensor simply scans through the fixed stress pattern. We can apply the chain rule to find the stress rate

$$\frac{\partial \sigma}{\partial t} = \frac{\partial \sigma}{\partial x} u \tag{3}$$

where terms in $dy/dt$ and $dz/dt$ have been omitted since the motion is in the $x$ direction only. Thus if the sliding speed $u$ is constant, the sensor signal is proportional to stress gradient in the direction of sliding. Integration of the stress rate across time will yield the stress distribution at the sensor depth along the test surface. Equation (3) also indicates that the sensor signal is proportional to the sliding speed $u$. While faster motion produces larger signals, increased sliding noise and the difficulties of controlling sensor height and velocity limit useful speeds.

*Impulse Responses:* Since the elasticity equations used here are linear, it is convenient to characterize the sensor's behavior in terms of impulse responses. It is simple to superpose the stress patterns generated by surface force distributions but not those generated by surface displacements, so the model

[1] In fact, the sensor effectively integrates conditions along the length of the piezofilm element. If plane strain conditions do not hold, the result will be the average value of the stress.

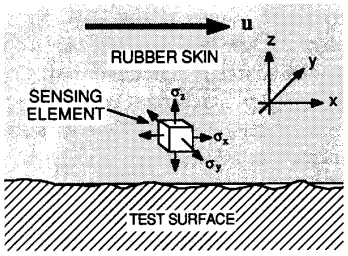


Fig. 4. Stress rate sensor coordinate system.

will be developed in terms of surface forces or "tractions." In this case the impulse response of interest maps from applied surface traction to measured stress distribution. In plane strain an impulse consists of a line load that has negligible width in the $x$ direction but is constant along the length of finger in the $y$ direction.

There are two different components of surface force that can be applied to the sensor surface in plane strain: a normal component in the $z$ direction perpendicular to the surface, denoted $p(x)$, and a shear component in the $x$ direction parallel to the surface, $q(x)$. There are three components of subsurface normal stress produced by each of these surface traction components. However, under plane strain conditions the stress in the $y$ direction is not independent; with Poisson's ratio = 1/2

$$\sigma_y(x,z) = \frac{\sigma_x(x,z) + \sigma_z(x,z)}{2}. \tag{4}$$

Thus there are four unit impulse responses that characterize the system[2]. The unit impulse response of $z$ stress due to the normal traction impulse of unit intensity per unit length in the $z$ direction $p(x) = \delta(x)$ is [16]

$$\sigma_z^p(x,z_0) = \left(\frac{-2}{\pi z_0}\right)\frac{1}{[1+(x/z_0)^2]^2}. \tag{5}$$

The response in $z$ stress for the shear impulse $q(x) = \delta(x)$ is

$$\sigma_z^q(x,z_0) = \left(\frac{-2}{\pi z_0}\right)\frac{(x/z_0)}{[1+(x/z_0)^2]^2} \tag{6}$$

and similarly, the unit impulse responses for $x$ stresses are

$$\sigma_x^p(x,z_0) = \left(\frac{-2}{\pi z_0}\right)\frac{(x/z_0)^2}{[1+(x/z_0)^2]^2} \tag{7}$$

and

$$\sigma_x^q(x,z_0) = \left(\frac{-2}{\pi z_0}\right)\frac{(x/z_0)^3}{[1+(x/z_0)^2]^2}. \tag{8}$$

These four impulses can be combined by making use of the fact that the finger is sliding. Under the assumptions of Coulomb friction, the ratio of the tangential force to the normal force for a sliding body is given approximately by the dynamic coefficient of friction $\mu = q(x)/p(x)$. This means that the surface tractions are at a fixed angle with the surface normal, so that in sliding the only direction in which tractions are applied to the finger surface is

$$\mathbf{r} = \hat{\mathbf{x}} + \mu\hat{\mathbf{z}} \tag{9}$$

where $\hat{\mathbf{x}}$ and $\hat{\mathbf{z}}$ are the unit vectors in the $x$ and $z$ directions. There is some difficulty with this assumption for rubber sliding over a surface with raised features; the coefficient of friction varies slightly with normal force and feature shape [26]. It is possible to circumvent this assumption entirely by constructing a more complicated sensor that measures several components of the stress distribution, as discussed in Section V. However, for present purposes this approximation produces acceptable results.

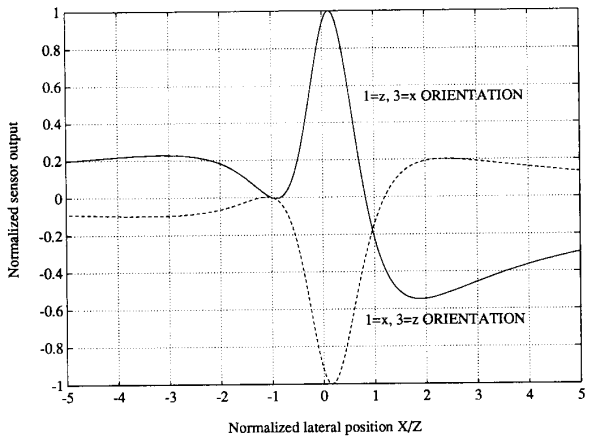


Fig. 5. Comparison of predicted sensor response to sliding impulse for different orientations of the piezofilm element ($\mu = 1$).

*Piezofilm Orientation:* Because the piezoelectric polymer has different piezoelectric constants in each direction, the orientation of the piezoelectric axes within the skin also must be considered. Since the plane strain model assumes that stress in the $y$ direction does not vary, the best performance is achieved by minimizing sensitivity to this component by orienting the 2-direction piezoelectric axis in the $y$ direction. The orientation of the 1- and 3-direction piezoelectric axes must then be specified in the $x - z$ plane. The piezoelectric constants in these directions are of the same order, so the choice of angle of orientation is somewhat arbitrary. Fig. 5 shows the shapes of the predicted sliding impulse responses for two orthogonal orientations, {1 to $x$, 3 to $z$} and {1 to $z$, 3 to $x$}, obtained by combining (2)–(9). Except for sign, the curves are essentially similar, so for ease of construction and improved durability the first of these orientations was selected so that the width of the piezofilm strip is parallel to the sensor surface.

*Impulse Response Equation and Integrated Signals:* Combining (2)–(9) and accounting for the piezofilm orientation, the sliding impulse response of the system can be

[2]Three components of shear stress are also produced by the surface tractions, but are difficult to measure and for the present purpose provide redundant information, so they will not be considered here.

written

$$g(x) = AR_f u \left(\frac{-2}{\pi z_0}\right) \frac{d}{dx}\left\{\left(d_3 + \frac{d_2}{2}\right)\frac{1+\mu(x/z_0)}{[1+(x/z_0)^2]^2} + (d_1 + \frac{d_2}{2})\frac{(x/z_0)^2 + \mu(x/z_0)^3}{[1+(x/z_0)^2]^2}\right\}. \quad (10)$$

Because of the derivative in this expression it is more convenient to work with the integral of the impulse response. Correspondence with the experimental results is easily obtained by integrating the sensor signal over the interval of interest. Variables corresponding to the integrated impulse response will be denoted with an "$i$" subscript. Thus the integrated sensor impulse response is

$$g_i(x) = \int_{-\infty}^{x} g(x')dx' \quad (11)$$

and the sensor signal integrated from the point $x_0$ is

$$v_i(x) = \int_{x_0}^{x} v(x')dx'. \quad (12)$$

*Implications of the Solid Mechanics Model:* Several general observations about the solid mechanics model should be noted. First, the above expressions give the stresses due to unit traction impulses, and the magnitude of the stress is proportional to the magnitude of the traction impulse. Thus for a given surface traction pattern the stress pattern will vary in proportion to the magnitude of the contact force, as expected for a linear model.

Second, each of the impulse responses ((5)–(8) and (10)) is expressed in terms of the dimensionless distance parameter $(x/z_0)$. This shows that the stress pattern simply scales with sensor depth: the stresses from concentrated surface tractions "spread out" with increasing depth in the elastic material. There is also a factor of $(1/z_0)$ in the leading term, indicating that the intensity of the stresses varies inversely with the sensing element depth. This means that the sensor resolution is roughly equal to the sensing element's depth beneath the elastic skin surface. As shown in Fig. 5, the impulse response width is about equal to one unit in the normalized $(x/z_0)$ coordinates. Although it is possible to extract surface information from the sensor signal at higher resolution (see section C), this is a convenient rule-of-thumb for characterizing the sensor's performance.

Another important point is that localized stresses correspond to high surface curvature. Thus the stresses measured by this sensor will be highest when the sensor skin is pressed against sharp edges and corners. This is a sort of automatic edge enhancement effect, which makes most tactile sensors (including human mechanoreceptors) very sensitive to surface discontinuities [10].

Finally, note that the elastic modulus of the finger material does not appear in these expressions. They describe stress (i.e., pressure) distributions due to applied forces, and the modulus enters only when displacements or strains are considered.

### C. Signal Processing

This section describes an algorithm for the inversion of the model predictions so that the surface traction distribution can be found from the sensor signal. Previous approaches to inversion problems in tactile sensing dealt with strain-based sensor signals and included linear filtering [8], [32] and analog neural networks [31] [22].

We will model the sensing process as a linear and space- and time-invariant system with additive noise. During sensing, the input to the system is the surface traction $r(x)$. The impulse response of the sensor $g_i(x)$ is convolved with the surface traction in the transduction process, resulting in the predicted signal $v_i(x)$. The sliding process adds noise $n_i(x)$, producing the measured signal $m_i(x)$

$$m_i(x) = r(x) * g_i(x) + n_i(x) \quad (13)$$

where $*$ denotes convolution.

The restoration process starts with the measured signal. A restoration filter with impulse response $h_i(x)$ is to be designed that takes into account the sensor response and the characteristics of the noise. Convolution of this filter function with the measured signal produces an estimate $r_{est}(x)$ of the surface traction

$$r_{est}(x) = m_i(x) * h_i(x). \quad (14)$$

Restoration filters are treated in many references on signal processing (e.g., [3], [21]. An often-used criterion for optimization of restoration filters is minimization of the mean squared error between the estimated and actual sensor inputs $\int_{-\infty}^{\infty} |r(x) - r_{est}(x)|^2 dx$. If, as is customarily assumed, the noise is additive, stationary, has zero mean, and is uncorrelated with the signal, then the Wiener filter provides the optimal inverse. The transfer function of this filter is

$$H_{opt} = \frac{G_i^*(s)}{|G_i(s)|^2 + |N_i(s)|^2} \quad (15)$$

where $G_i^*(s)$ is the complex conjugate of the sensor transfer function and $|N_i(s)|^2$ is the noise power spectrum, and all of these functions are in appropriately normalized form.

The function of the Wiener filter can be explained by reference to Fig. 6, which shows the power spectra of the sensor response, the typical sliding noise, and the Wiener filter as a function of spatial frequency. The sensor power spectrum decreases rapidly with increasing frequency. Equation (10) shows that the stress distribution spreads out with increasing sensor depth, so that the sensor acts as a low pass filter to effectively "blur" the surface tractions. The Wiener filter compensates for this effect by increasing its gain as the frequency increases. The product of the sensor response and the restoration filter then approximates a flat response. However, at high frequencies the sliding noise becomes larger than the sensor signal, so the gain of the Wiener filter decreases. Thus noise characteristics set the fundamental limit to the highest spatial frequencies that can be recovered. Experimental evaluation of the performance of this filter is presented in Section IV-B.

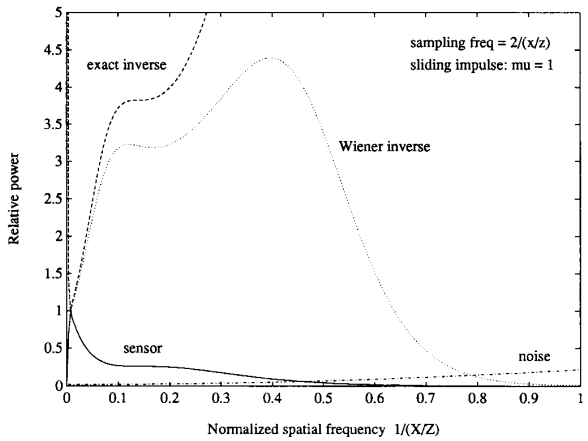


Fig. 6. Power spectra of the sensor impulse response and inverse filters.

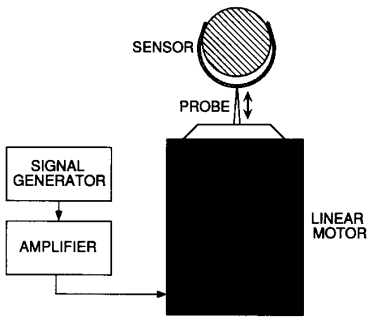


Fig. 7. Apparatus for measuring the response of the stress rate sensor.

## IV. Experimental Results

This section presents experimental measurement of the sensor's performance. Further details of the sensor tests can be found in [14].

### A. Basic Sensor Performance

One problem with testing a dynamic tactile sensor is the inability to perform static tests of the sensor's response: a stimulus pressed statically against the sensor surface generates no signal. In particular, it is difficult to assess the spatial impulse response of the sensor without sliding over surface features. Since this is precisely the process that must be independently calibrated, another means of characterizing the response is required. Thus the apparatus shown in Fig. 7 was used to characterize the basic performance of the stress rate sensor. A knife-edge probe is attached to the moving stage of a linear motor and aligned parallel with the piezoelectric element. The probe is pressed against the surface of the sensor and displaced sinusoidally in the normal ($z$) direction. Both the amplitude and the frequency of the motion can be precisely controlled. In addition, the motor and probe are mounted on a linear translation stage so that the spatial variation of the sensor response in the $x$ direction may be measured.

The temporal bandwidth range of interest is limited by spatial resolution requirements. The highest useful frequency

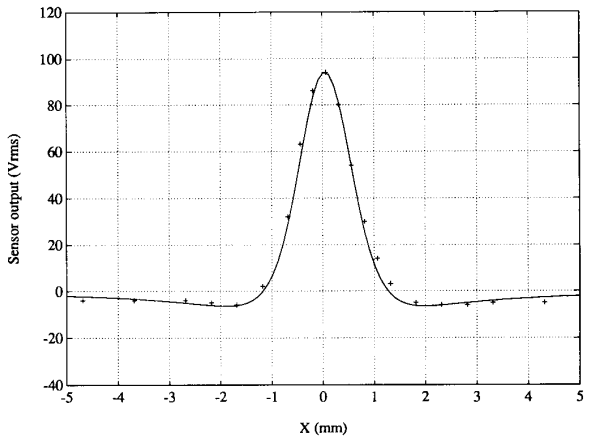


Fig. 8. Quasi-static measurement of the stress rate sensor's response for a normal impulse and the theoretically predicted curve. Negative values of sensor output indicate a 180 degree phase shift with respect to the phase at $x = 0$.

can be estimated by dividing the largest expected sliding speed (10 cm/s) by the smallest resolution (0.1 mm $\ll z_0$), yielding 1000 Hz. The apparatus shown in Fig. 7 was used to measure frequency response from 10 to 1000 Hz. The results show the expected +12 dB per octave slope and 90 degree phase shift, confirming that the sensor measures the derivative of the applied stress. The same setup was used to test the linearity of the sensor with respect to the magnitude of the input signal. The sensor output is within 3 dB of linear across the two orders of magnitude tested.

The apparatus shown in Fig. 7 was also used to measure the spatial impulse response. The probe edge was brought into normal contact with the sensor surface at a sequence of locations in the $x$ direction. The vibration of the probe served to maintain output from the sensor so that the magnitude of the integrated impulse response could be measured at each location. Fig. 8 shows the impulse response and the theoretically predicted curve from (10). The amplitude of the theoretical curve has been fitted to the experimental data and the width of the piezofilm strip has been taken into account by convolving the calculated curve with a rectangular window 0.7 mm wide. The calculated and experimental curves show close agreement, indicating that the development presented in Section III is successful in modeling the sensor's behavior despite the model's idealizations. Similar close agreement with theoretical prediction is obtained with the probe oriented at 45 degrees, indicating successful modeling of the response to shear tractions [14].

Next the sensor was tested with a sliding impulse. A raised metal edge was attached to a turntable so that the indentation distance and sliding speed could be repeatably controlled. A typical integrated sensor signal is shown in Fig. 9. This waveform shows significant differences from both the theoretical curve and from the quasi-static measurements shown above. The size of the leading lobe has been reduced and some of the high-frequency details have been blurred. This is apparently due to unmodeled effects of the sliding process. In particular, during sliding different regions of the

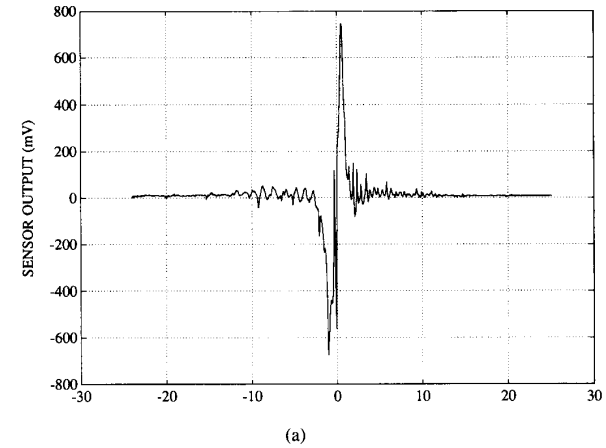


(a)

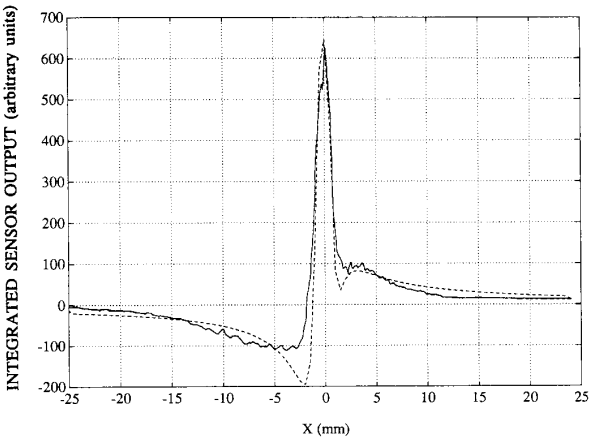


(b)

Fig. 9. Measured sensor response to a sliding impulse. (a) Stress rate sensor signal as a raised metal edge passes across the sensor surface; (b) the integral of the sensor signal and the corresponding theoretical response calculated with (10).

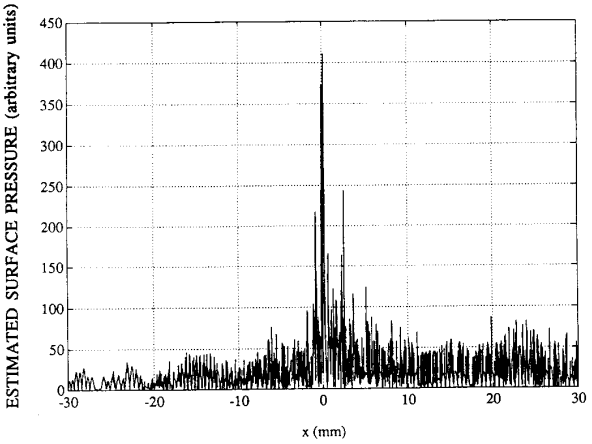


Fig. 10. Sliding surface traction estimate calculated with the Wiener filter based on the theoretical impulse response. Sensor data as shown in Fig. 9.

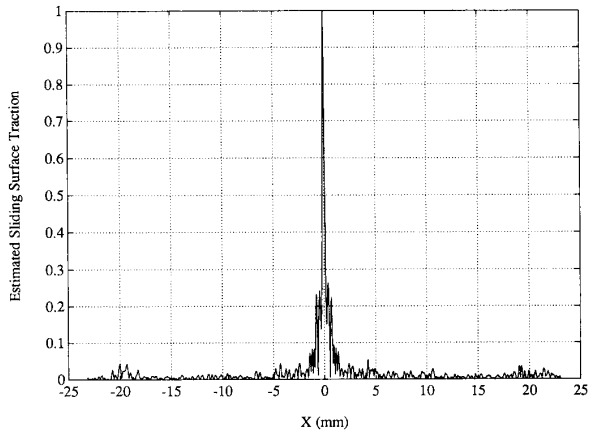


Fig. 11. Sliding surface traction estimate calculated with the Wiener filter based on the measured impulse response. Sensor data as shown in Fig. 9.

sensor surface may experience rapidly varying shear loads as small regions in the contact area momentarily stick and then release. The stress rate sensor responds strongly to the resulting changes in stress within the rubber. The piezofilm element does not remain in precise alignment as it did during the quasi-static impulse response tests described above, which violates the plane strain assumption. This limits peak stress values and blurs high frequency features, as evidenced in the power spectrum of the measured impulse response. Such dynamic sliding effects pose a fundamental limit to the success of the model, although the theoretical response is reasonably correct and useful in understanding the sensor's function.

### *B. Inverse Filtering*

Fig. 10 reveals that the Wiener filter encounters difficulties in accurately reconstructing the surface traction distribution. The filter is designed to compensate for the theoretical sensor response in the presence of noise uncorrelated with the signal. The differences between the predicted and measured responses as seen in Fig. 9 are repeatable and thus represent inaccuracies in the modeled response, or "correlated noise," which the Wiener filter is not able to correct.

One alternative for improving the performance of the reconstruction process is to use an empirically derived impulse response rather than the theoretical one. To test this approach, a filter design was based on the experimentally measured impulse response averaged over a number of readings to remove uncorrelated noise. This limited the degradation due to the unmodeled sliding effects. This version of the Wiener filter produced good estimates of the surface traction (see Fig. 11), as expected since it was designed with the measured system response. This demonstrates that the stress rate sensor produces repeatable signals despite the presence of unmodeled sliding effects and considerable noise.

### *C. Resolution Limits*

For this sensor there are two different resolution limits which must be distinguished: one is the feature height and the other is the lateral extent of the feature; these limits will in general be quite different. Once again, from (10) the stress pattern's width decreases and the magnitude increases as the

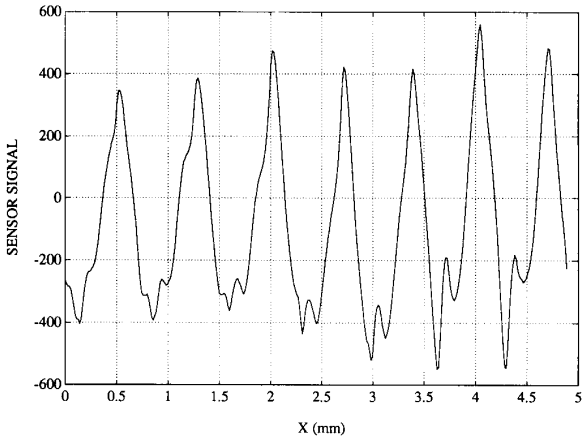


Fig. 12. Integrated stress rate sensor output while traversing 6.5-$\mu$-high ridges.

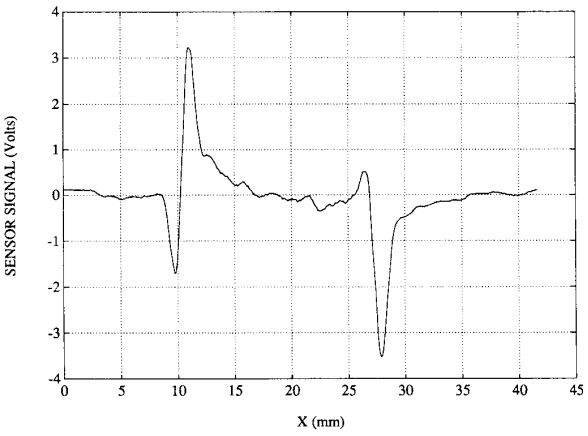


Fig. 13. Integrated sensor signal as the tape slides onto and then off a piece of cellophane tape.

sensor depth $z_0$ decreases. Thus placing the piezofilm sensing elements as close to the surface as possible serves to increase resolution in both feature width and feature height.

Resolution limits in the reconstruction process are also important. Fearing [8] investigated the use of linear inverse filtering to reconstruct surface pressure distributions from tactile array data. Array sensors have limited spatial sampling capability ($7 \times 8$ elements in Fearing's work), so the results of the inversion were unsatisfactory due to aliasing. In the case of the stress rate sensor, difficulties with aliasing do not arise because it is possible to densely sample the subsurface stress distribution during sliding. Thus resolution in the reconstructed surface traction is limited by noise in the sliding process, as discussed above. Since the magnitude and spectral characteristics of the noise vary from surface to surface, an adaptive inverse filter (e.g., a Kalman filter) that takes these noise variations into account would permit optimization of the reconstruction process in real time for a variety of surfaces.

As an extension of the inversion process, it is interesting to note that Fearing succeeds in finding the radius and orientation of cylinders far smaller than the linear resolution limit of the sensor would seemingly allow. This approach works because it presupposes the cylindrical form of the object, so that the radius and orientation parameters can be "fitted" to the data. Similarly, the stress rate sensor perception limits can be significantly smaller than the linear limit if something is known of the stimulus in advance. In particular, this strategy could be used to find the shape of fine surface features from estimated surface traction data [8] [9].

Because the stress rate sensor is capable of detecting extremely fine features, it is difficult to create appropriate stimuli to experimentally test its performance limits. For similar purposes researchers in human tactile sensing have created patterns of raised ridges and dots on smooth glass plates with submicron precision using integrated circuit fabrication techniques [15]. The stress rate sensor was tested with one such plate obtained for this purpose [18]. The pattern consists of a series of raised, parallel, rectangular ridges 6.5 $\mu$ high, 50 $\mu$ wide, and 12 mm long on 700 $\mu$ centers. The stress rate sensor was lightly stroked over the glass plate across the ridges at about 1.4 cm/s. Fig. 12 shows the recorded signal. Each ridge produced a large, distinct peak. Because the ridge spacing was somewhat smaller than the linear resolution limit and because there was substantial sliding noise, the linear restoration technique is not capable of reproducing the square-edged ridge profile, although the fundamental spatial frequency is readily reproduced. It is clear from this test that the 6.5-$\mu$ height is well within the height detection capabilities of the sensor, and given the magnitude and clarity of this signal, the minimum detectable height may be an order of magnitude smaller [15] [18].

### *D. A Fine Feature Detection Task*

As a more or less practical application of the stress rate sensor, consider the task of locating the free end of a roll of cellophane adhesive tape that has become reattached to the roll. Since the tape is transparent and very thin, it is quite difficult to locate visually, and this is one task in which most people prefer to use their sense of touch. Locating this sort of minute surface discontinuity is easy for the stress rate sensor, although detection of the tiny displacement difference is beyond the capabilities of traditional tactile array sensors.

Fig. 13 shows the signal as the stress rate sensor traverses a piece of tape 50 $\mu$ thick and 15 mm wide. On the ascending edge (leftmost in Fig. 13) the signal has large positive and negative peaks. The antisymmetric form of this signal indicates that shear forces are present (cf. (6) and (8)) due to the rubber catching on the leading edge of the tape. On the descending edge the waveform is closer to symmetrical, implying that the shear component of the surface traction has decreased relative to the normal component. The rubber skin slides smoothly off the tape without catching, effectively reducing the local coefficient of friction. Thus the stress rate sensor can provide information about local contact conditions such as the coefficient of friction as well as fine features and textures. Such variations in contact conditions can be important in manipulation, and dynamic tactile sensors can contribute to the reliability and robustness of manipulation by monitoring these conditions [13].

## V. Discussion and Extensions

### A. Inferring Shape from Estimated Surface Tractions

The restoration algorithm described in Section III. estimates the surface traction distribution from the measured subsurface stress rates. These surface tractions are of considerable importance in applications such as manipulation where local contact force information is crucial. In addition, it would be useful to find the surface displacements corresponding to the tractions and thus the shape of the surface features.

Unfortunately, calculating displacements from the stress rate sensor signal is not straightforward. Elasticity theory provides a means for determining surface displacements from subsurface stresses [30], but knowledge of the shear stress or shear strain distribution is required. Nonetheless, it is possible to at least classify surface features based on stress rate sensor data. The stress rate sensor responds strongly to features with high curvature, such as ridges and edges. One example set of features to be classified might consist of very narrow raised ridges (such as the sliding impulse, Fig. 9) and leading and trailing step edges (such as the cellophane tape example, Fig. 13). Comparison of these figures shows that a distinct signal is produced by each of these prototypical features. Thus pattern recognition techniques should permit differentiation of these feature types. In addition, if the basic form of the surface feature is known it should be possible to "fit" the parameters of the feature (such as curvature) to the data. This is the same approach used successfully by Fearing to find the radius and orientation of a cylinder from tactile array data [8], [7].

A straightforward extension of the approach used here can permit the relaxation of the constant friction assumption in the foregoing analysis. For plane strain this assumption reduced the inversion problem to one dimension so there was only one quantity to be recovered from the sensor data, the traction in the $\mathbf{r}(\mathbf{x})$ direction. As shown above, it is possible to recover this quantity by sensing only one variable, the stress rate signal $m_i(x)$. But if the pressure and shear tractions are taken to be independent then at least two independent subsurface stress rates must be measured. This can be accomplished by incorporating two piezofilm elements with different orientations. Fig. 5 illustrates the impulse responses for two elements oriented at right angles. Calculations confirm that it is possible to extract the distinct stress components $\sigma_x$ and $\sigma_z$ from these signals, and restoration filters can be constructed following the procedure outlined in Section III. Using this approach it should be possible to recover the separate components of traction under plane strain conditions by using two sensing elements.

### B. Multiple Sensing Elements

One important characteristic of the stress rate sensor prototype described here is its directional sensitivity. Extended features oriented perpendicular to the direction of sliding are readily detected, while those oriented parallel to the sliding direction produce no output. This limitation can be overcome through suitable construction and use of the sensor. First, a set of sensors with different orientations can be combined in a single fingertip so that at least one sensor will be nearly normal to any scanning direction. Second, the fingers can be scanned in small circular motions about an area of interest. Thus at some point in each scanning cycle the fingertip motion will bring any extended surface feature perpendicularly across an appropriately oriented sensor element. Then once a feature is detected it may be scanned repeatedly in a variety of directions to provide additional information about it. Apparently human texture perception is also dependent on the relative direction of fingertip motion and surface pattern orientation, perhaps because of the ridge structure of human fingerprints [20]. It is also possible to augment the sensor design by including additional piezofilm elements so that the full three-dimensional subsurface strain pattern can be measured. DeRossi *et al.* [5] have proposed schemes for inverting such signals to find extended contact properties.

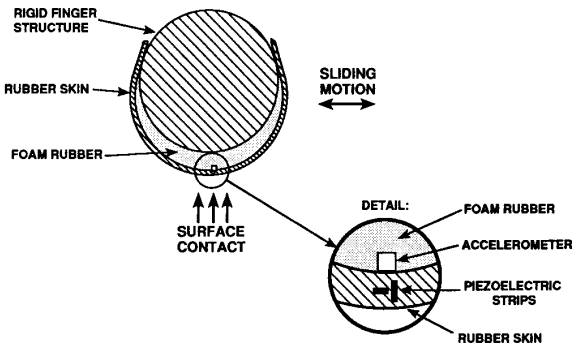


Fig. 14. Cross section of a robot finger with both skin acceleration and stress rate sensors. The detail shows the accelerometer mounted on the inside of the rubber skin, which also contains piezoelectric strips for stress rate sensing.

Multiple sensing elements that lie along the same line of travel are also of interest. To some extent such elements convey redundant information because they scan over the same part of the object surface. But by correlating the signals from these elements the effective noise level in the sensor signals can be reduced. In addition, the uncorrelated portions of the signals contain information about the tendency of the skin to catch and snap back during sliding. This reveals characteristics of the texture of the object surface as well.

Further information about fine textures can be obtained by combining the stress rate sensor with another dynamic tactile sensor, the skin acceleration sensor [12]. This sensor uses a small accelerometer attached to the inner surface of the rubber skin to provide information about minute vibrations in the contact area. It provides information about contact conditions during manipulation such as the onset of slip or the making or breaking of contact. It can be used in the same manner as the stress rate sensor, and can be readily combined in the same robot finger, as shown in Fig. 14.

Generally, "texture" refers to the combination of a number of small-scale distributed surface properties, including small surface features, compliance, thermal properties, and surface contamination. Humans perceive a surface as textured rather than perceiving each small surface feature individually if the features are less than about 1 mm in extent, and texture sensing requires that the fingers move over the surface. Surface

textures can have a great influence on frictional properties, particularly on wet or dirty surfaces [4]. Tactile sensing of textures is also important for object recognition and can aid in the interpretation of visual images.

Dynamic tactile sensors are well suited to texture perception. They respond to high spatial and temporal frequencies, and by sliding over surfaces they produce shear tractions which provide additional information about small surface asperities. However, they are not capable of accurately measuring extremely fine surface geometry. High frequency noise limits the ability of the stress rate sensor to reconstruct the highest spatial frequencies. Likewise, the large active area and resonant behavior of the skin acceleration sensor precludes its use in extracting spatial information. Nevertheless, preliminary experimental tests show large variations in the signals from these sensors for different surface textures. Further investigation of the ability to classify various textural properties is planned. In particular, it appears that these sensors can be combined to yield multiple-parameter information about textures that would be impossible to obtain with either sensor alone.

Finally, it is important to note that the sensor can be used in "nonlinear" ways in manipulation tasks. For example, when the finger first makes contact with an object the stress distribution within the fingertip skin varies rapidly. Similarly, small slips at the edge of the contact area just before a grasped object begins sliding produce rapid stress transients. Because it is particularly sensitive to these small, fast changes in stress, the stress rate sensor can be used to detect these phenomena. In many cases a simple threshold technique will be sufficient. Since these phenomena represent important transitions in the mechanical state of the hand-object system, this sensor can be used to improve the robustness of robotic manipulation in a range of tasks [13].

## VI. Conclusion

Most tactile sensing research has been directed at static measurement of object shape, but other parameters, including fine features, surface texture, friction, and contact conditions are important as well. Dynamic tactile sensors are designed to measure these properties by taking advantage of sensor motion. As with human touch sensing, motion provides fundamentally different information by changing the way the sensor interacts with the environment. Motion also permits a surface to be scanned at high resolution using a small number of sensors. Because the stimulus is constantly changing during motion, measurements can be made in terms of derivative quantities. These derivative quantities produce large, fast signals that convey information about *changes* in surface properties and contact conditions.

The stress rate sensor uses piezoelectric polymer elements to measure changes in stress beneath the surface of the rubber skin covering the sensor. By modeling the interaction between the sensor and environment in terms of linear elasticity theory it is possible to use a linear deconvolution filter to find the distribution of forces at the surface of the sensor. While this model is based on a number of idealizations, it is successful in predicting the experimental results. Furthermore, it provides a means of reasoning about and optimizing the sensor design and suggests extensions of the interpretation process. The next challenge is to integrate this sensor with other sensing modalities and test its utility in real manipulation and exploration experiments.

## Acknowledgment

We would like to thank Ronald Fearing for helpful discussions and Robert LaMotte for providing the etched glass plate used to test the sensor's resolution limits.

## References

[1] P. K. Allen, *Robot Object Recognition Using Vision And Touch*. Boston: Kluwer Academic, 1987.
[2] G. Buttazzo, P. Dario, and R. Bajcsy, "Finger based explorations," in *Intelligent Robots and Computer Vision: Fifth in a Series*, D. Casasent, Ed., *Proc. SPIE*, vol. 726, Cambridge, MA, Oct. 28–31, 1986, pp. 338–345.
[3] K. R. Castleman, *Digital Image Processing*. Englewood Cliffs, NJ: Prentice-Hall, 1979.
[4] M. R. Cutkosky, J. M. Jourdain, and P. K. Wright, "Skin materials for robotic fingers," in *The Proc. 1987 IEEE Int. Conf. Robotics Automat.*, vol. 3, Mar. 31–Apr. 3, 1987, pp. 1649–1654.
[5] D. DeRossi *et al.*, "Fine-form tactile discrimination through inversion of data fram a skin-like sensor," In *The Proc. 1991 IEEE Int. Conf. Robotics Automat.*, Sacramento, CA, Apr. 1991, pp. 398–404.
[6] R. E. Ellis, "Acquiring tactile data for the recognition of planar objects," in *Proc. 1987 IEEE Int. Conf. Robotics Automat.*, Mar. 31–Apr. 3 1987, pp. 1799–1805.
[7] R. S. Fearing, "Tactile sensing for shape interpretation," in *Dextrous Robot Hands*, S. T. Venkataraman and T. Iberall, Eds. New York: Springer-Verlag, 1990, ch. 10, pp. 209–238.
[8] ——, "Tactile sensing, perception and shape interpretation," Ph.D. dissertation, Stanford Univ., Stanford, CA, 1987.
[9] ——, "Tactile sensing mechanisms," *Int. J. Robotics Res.*, vol. 9, no. 3, pp. 3–23, June 1990.
[10] R. S. Fearing and J. M. Hollerbach, "Basic solid mechanics for tactile sensing," *Int. J. Robotics Res.*, vol. 4, no. 3, pp. 40–54, 1985.
[11] W. E. L. Grimson and T. Lozano-Perez, "Model-based recognition and localization from sparse range or tactile data," *Int. J. Robotics Research*, vol. 3, no. 3, pp. 3–35, Fall 1984.
[12] R. D. Howe and M. R. Cutkosky, "Sensing skin acceleration for texture and slip perception," in *Proc. 1989 IEEE Int. Conf. Robotics Automat.*, Scottsdale, AZ, May 1989, pp. 145–150.
[13] R. D. Howe, N. Popp, P. Akella, I. Kao, and M. Cutkosky, "Grasping, manipulation, and control with tactile sensing," in *Proc. 1990 IEEE Int. Conf. Robotics Automat.*, Cincinnati, OH, May 1990, pp. 1258–1263.
[14] R. D. Howe, "Dynamic tactile sensing," Ph.D. dissertation, Stanford Univ., Stanford, CA, Oct. 1990.
[15] R. S. Johansson and R. H. LaMotte, "Tactile detection thresholds for a single asperity on an otherwise smooth surface," *Somatosensory Res.*, vol. 1, no. 1, pp. 21–31, 1983.
[16] K. L. Johnson, *Contact Mechanics*. New York: Cambridge University Press, 1985.
[17] R. L. Klatzky, R. Bajcsy, and S. J. Lederman, "Object exploration in one and two fingered robots," in *Proc. 1987 IEEE Int. Conf. Robotics Automat.*, 1987, pp. 1806–1809.
[18] R. LaMotte, private communication, 1990.
[19] R. H. LaMotte and M. A. Srinivasan, "Surface microgeometry: Tactile perception and neural encoding," in *Information Processing in the Somatosensory System*, O. Franzen and J. Westman, Eds. New York: Macmillan, 1990.
[20] S. J. Lederman and D. T. Pawluk, "Lessons from the study of biological touch for robot tactile sensing," in *Advanced Tactile Sensing for Robotics*, H. Nichols, Ed. London: World, 1992.
[21] A. Papoulis, *Signal Analysis*. New York: McGraw-Hill, 1977.
[22] Y. C. Pati, D. Friedman, P. S. Krishnaprasad, C. T. Yao, and M. C. Peckerar, "Neural networks for tactile perception," in *The Proc. 1988 IEEE Int. Conf. Robotics Automat.*, Philadelphia, PA, 1988, pp. 134–139.
[23] R. W. Patterson and G. E. Nevill, Jr., "The induced vibration touch sensor—A new dynamic touch sensing concept," *Robotica*, vol. 4, pp. 27–31, 1986.

[24] Penwalt, *KYNAR Piezo Film Technical Manual*, Penwalt Corp., King of Prussia, PA, 1983.
[25] J. R. Phillips and K. O. Johnson, "Tactile spatial resolution III: A continuum mechanics model of skin predicting mechanoreceptor responses to bars, edges and gratings," *J. Neurophysiology*, vol. 46, no. 6, pp. 1204–1225, Dec. 1981.
[26] A. Schallamach, "Friction and abrasion of rubber," *Wear*, vol. 1, pp. 384–417, 1957.
[27] T. H. Speeter, "Analysis and control of robotic manipulation," Ph.D. dissertation, Case Western Reserve University, 1987.
[28] S. A. Stansfield, "A robotic perceptual system utilizing passive vision and active touch," *The Int. J. Robotics Research*, vol. 7, no. 6, pp. 138–161, Dec. 1988.
[29] M. M. Taylor, S. J. Lederman, and R. H. Gibson. Tactual perception of texture, in E. C. Carterette and M. P. Friedman, Eds., *Handbook of Perception Vol. 3*, ch. 12, pp. 251–272. New York: Academic, 1973.
[30] S. Timoshenko and J. N. Goodier, *Theory of Elasticity*. New York: McGraw–Hill, 1951.
[31] A. J. Worth and R. R. Spencer, "A neural network for tactile sensing: The Hertzian contact problem," in *Int. Joint Conf. Neural Networks*, pp. I–267–274, 1989.
[32] R. Yang, "Tactile perception for multifingered hands," Tech. Rep. SRC TR 87-162, Syst. Res. Center, Univ. Maryland, College Park, MD, 1987. (Also Masters thesis, Univ. Maryland, 1987.)

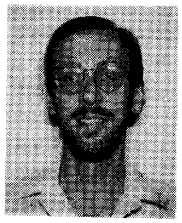

**Robert D. Howe** received the B.A. degree in physics in 1979 from Reed College and the Ph.D. degree in 1990 from Stanford University, Stanford, CA.

He is currently an Assistant Professor of Mechanical Engineering in the Division of Applied Sciences at Harvard University, Cambridge, MA. He worked in the electronics industry as a design engineer for several years before earning his doctoral degree. His research interests include robotic manipulation, tactile sensing and display, teleoperation, and biomechanics.

**Mark R. Cutkosky** received the B.S. degree in mechanical engineering in 1978 from the University of Rochester, and the M.S. and Ph.D. degrees in 1985 from Carnegie-Mellon University, Pittsburgh, PA.

He is an Associate Professor in the Design Division of the Mechanical Engineering at Stanford University, Stanford, CA. He joined the Design Division in 1985, after working for several years in the Robotics Institute at Carnegie–Mellon University, Pittsburgh, PA, and as a Design Engineer at ALCOA, Pittsburgh. His work at Carnegie–Mellon included the development of robotic end-effectors, the design and control of automated manufacturing cells and dextrous manipulation with robotic wrists and hands. He is an Associate Technical Editor for the *ASME Transactions: Journal of Engineering for Industry*. His recent work in robotics has focused on the use of tactile information to facilitate manipulation with sliding and rolling. In other work, he has been developing computer-aided systems for concurrent design and process planning of electromechanical devices.

Dr. Cutkosky is an NSF Presidential Young Investigator and the Anderson Faculty Scholar at Stanford University. He is a member of ASME, SME, and Sigma Xi.